PROCEEDINGS OF SCIENCE

Blazars: an updated review

Luigi Costamante*
ASI - Italian Space Agency, Unità Ricerca Scientifica
E-mail: `luigi.costamante@asi.it`

I give an overview on recent advances in our understanding of the blazar phenomenon. I focus in particular on results provided by the new generation of large-area GeV and TeV telescopes, which have revealed several new aspects of blazars structure and emission properties. On the one hand, the blazar-sequence scenario seems confirmed in its main features, although with differences between FSRQ and BL Lacs. Yet it remains uncertain if it is real or caused by selection biases. On the other hand, several other results are challenging the standard emission models, like the absence of the cut-off in the gamma-ray spectrum expected if produced inside the Broad Line Region, the existence of extreme-TeV BL Lacs with gamma-ray emission peaking at multi-TeV energies, and ultrafast variability on scales much less than the size of the black hole. This review does not aim to be exhaustive nor complete, but to provide an update on some main topics from observational results emerged in the last years.

Multifrequency Behaviour of High Energy Cosmic Sources - XIII - MULTIF2019
3-8 June 2019
Palermo, Italy

---

*Speaker.

1. Introduction

About 10% of Active Galactic Nuclei (AGN) display relativistic jets which produce radiation over the whole electromagnetic spectrum, from radio to TeV energies. When the jet is pointing at us, the source is called a blazar, and the spectral energy distribution (SED) is dominated by the beamed emission of the plasma moving relativistically in the jet.

Relativistic jets are among the most powerful phenomena in the Universe: besides radiation, which can reach an apparent luminosity in excess of 10^{49} erg/s, the jet power necessary to supply the lobes must be of the order of 10^{44-47} erg/s for millions of years, to explain the existence of the radio lobes and their total energy content of 10^{59-61} erg [1, 2]. Gamma-ray transparency arguments and the apparent superluminal motion with speed up to $40-50c$ –which provides a lower limit to the bulk-motion Lorentz factor Γ– requires Lorents factors of $\Gamma \simeq 10-50$.

While blazars are the most extreme (and probably efficient) bulk accelerators, they are not extreme *particle* accelerators like pulsars or SNRs: even in sources with an observed synchrotron emission peaking close to 100 keV, the particle acceleration rate remains 4-5 orders of magnitude less than its maximum possible rate (when a particle gains all its energy in 1 gyroradius).

The mechanism by which jets are launched is not yet well known. The new results from the Event Horizon Telescope on M87 [3] might yield some new clues in this respect. Their precise composition is uncertain as well, but most of the kinetic power required to feed the lobes must be provided by protons, otherwise the Compton drag on a pairs-dominated jet would effectively decelerate and stop the jet (see e.g. [4]). A composition of no more than ~10 pairs per proton seems allowed [5].

The two most likely sources of jet power are the gravitational energy of the accreting matter or the rotational energy of the spinning black hole (BH). We now know that the former is not sufficient: at least part of the power must come from the BH spin energy, because the total jet power calculated from radiation (assuming 1 cold proton per emitting lepton) is in most sources higher than the total accretion luminosity $\dot{M}c^2$ [6], in agreement with general relativistic MHD simulations [7, 8].

The likely association of a blazar with a high-energy neutrino event and higher neutrino flux [9, 10, 11] is exciting but presents new problems. PeV neutrinos mark the presence of ultrarelativistic protons with energy ~20 times higher, and the contribution to the jet total power can go from a few to a few thousand times the previous estimates, depending on the emission mechanism. Neutrinos are generated only by hadronic processes. The most efficient production mechanism for the jet is the photomeson production, where protons interact with ambient target photon fields. Blazars can have dense photon fields, but the high photon densities required for an efficent and copious neutrino production tend to make the source opaque to gamma-rays, killing the gamma-ray/neutrino connection which is itself at the basis of the association of the blazar TXS 0506+056 with the IceCube neutrino detection. Curiously, this source is an intermediate blazar in almost every sense: SED type, overall luminosity, broad emission lines which could classify it as a FSRQ as well as a BL Lac (see e.g. [12]). Therefore it does not provide any indication if neutrino production is more likely in FSRQ/LSP or BLLac/HSP objects. This topic is still highly debated, and here I leave its discussion to the other ad-hoc contributions in this conference (e.g. by Righi et al. and Padovani et al.).

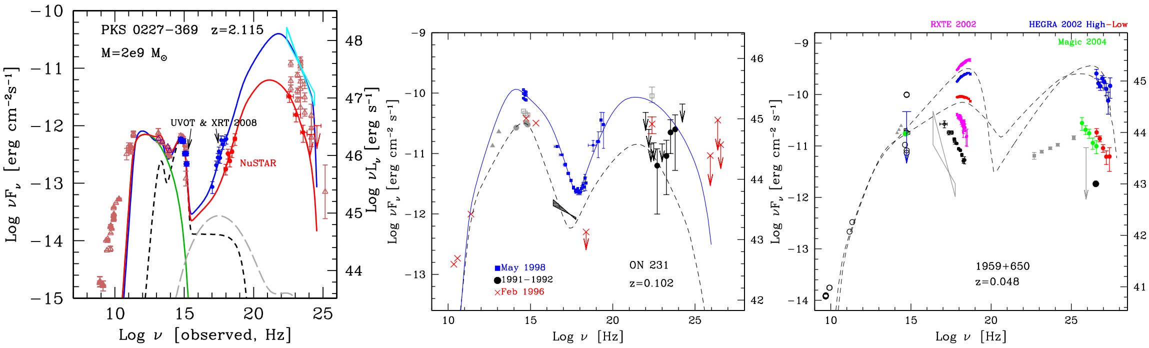

Figure 1: SEDs of 3 type of blazars representative of LSP-type FSRQ (left), ISP-type (center) and HSP-type (right) BL Lacs. Note that for LSP-type SEDs, the accretion disk emission (and torus) can become clearly visible in the IR-to-UV range. In ISP the X-ray spectrum is concave from the presence of both emission components (synchrotron and gamma-ray humps). In HSP the X-ray spectrum is fully dominated by synchrotron radiation, and can become hard during flares when the peak shifts to extreme energies. Figures or data from refs. [13, 14, 15].

2. Main blazars properties

All blazars are characterized by two broad humps in the SED, peaking at low and high energies (see Fig. 1). They are commonly (but not uniquely) explained so far as synchrotron and inverse Compton (IC) emission from a population of relativistic electrons in the jet. The origin of the seed photons for the IC scattering marks the difference among leptonic scenarios: synchrotron photons produced by the same electrons (Synchrotron Self-Compton mechanism, SSC) or by other parts of the jet (e.g. spine-layer/spine-sheath scenarios), or photons from radiation fields outside the jet (External Compton, EC), such as optical-UV photons from the Broad Line Region (BLR) or infrared radiation from the dusty torus [16, 17].

Blazars can be classified according to two main properties: thermal emission (from BLR, disk and torus) and non-termal emission (from the jet). From optical spectroscopy, blazars are historically divided in flat-spectrum radio quasars (FSRQs) and BL Lac objects (BL Lacs), with the former displaying strong, broad emission lines like radio-quiet quasars, and the latter showing weak emission lines or completely featureless spectra [18]. The dividing line has been historically put at 5Å equivalent width. Since this definition is based on a ratio between line and continuum, with both being variable, there is a significant overlap between the two classes, and a percentage of sources are likely mis-classified due to the jet emission swamping the thermal emission of the lines and the disk (so-called “masquerading BL Lacs" [19]). Despite this, there is a real and substantial difference between FSRQ and BL Lacs: true BL Lacs have intrinsicaly very faint or no line emission (with luminosities orders of magnitude lower than in FSRQ), weak or no torus emission and an underluminous accretion disk. On the contrary, powerful FSRQs have highly luminous disks, torus and emission lines. The recent estimates of black hole masses for a large number of objects allow the estimates of luminosities in Eddington units. The separation between the two classes seems to occur at $L_{disk}/L_{Edd} \sim 10^{-2}$ [20], likely marking the transition between a radiatively efficient, geometrically thin, optically thick accretion flow [21] and a radiatively inefficient, geometrically thick, optically thin accretion flow [22]. Therefore, new more physical definitions for “real" FSRQs and

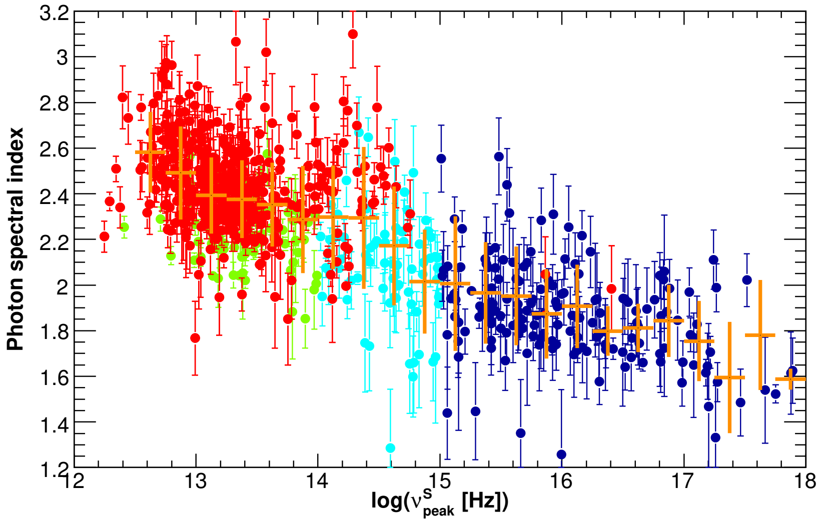

Figure 2: *Fermi*-LAT photon index as a function of the synchrotron peak frequency ν_{peak}, as calculated from polynomial fits to the SED [25]. Red: FSRQs, green: LSP BL Lacs, cyan: ISP BL Lacs, dark blue: HSP BL Lacs. The orange bars show the average index for different bins in ν_{peak}. From ref. [25]

BL Lacs have been recently introduced, related to the line luminosity in Eddington units (above or below 10^{-3}) [23], or on the line composition: namely objects with or without high-excitation emission lines in their optical spectra, as in high-excitation (HEGs) and low-excitation (LEGs) galaxies, respectively [24].

The blazars jet emission spans a wide range of SED peak frequencies, going from mm to X-ray energies for the synchrotron peak, and correspondingly from MeV to TeV energies for the high-energy peak. Blazars are thus divided in “Low-", “Intermediate-" and “High-synchrotron peaked" sources (LSP, ISP and HSP, see [26, 25]), according if the synchrotron $\nu_{peak} < 10^{14}$ Hz (< 0.41 eV), between 10^{14} Hz and 10^{15} Hz ($0.41 - 4.1$ eV), or $> 10^{15}$ Hz (> 4.1 eV). Figure 1 illustrates the different SEDs representative of these three types of blazars.

The main and most direct observational feature characterizing the SED classification is the 0.1-10 keV X-ray spectrum. In LSP objects, it is fully dominated by the second hump emission (i.e. the IC emission of low-energy electrons, in the leptonic scenario). In these objects the optical band is located near the minimum of the beamed jet emission (i.e. the valley between the two SED humps), and thus the emission from the accretion disk (and possibly the torus) can emerge and become clearly visible. This is often the case for powerful FSRQ, allowing a direct measure of the accretion disk parameters and BH mass [27].

The signature of intermediate sources is instead a concave X-ray spectrum [14], where we observe directly the transition between the two SED humps (i.e. between the tail of the synchrotron emission and the start of the IC emission, from the highest and lowest-energy electrons respectively).

In HSP sources, the X-ray spectrum is fully dominated by the synchrotron emission of high-energy electrons, with a generally steep slope which can become again hard as in LSP objects but this time due to the synchrotron peak passing over and beyond the observed X-ray band. In the

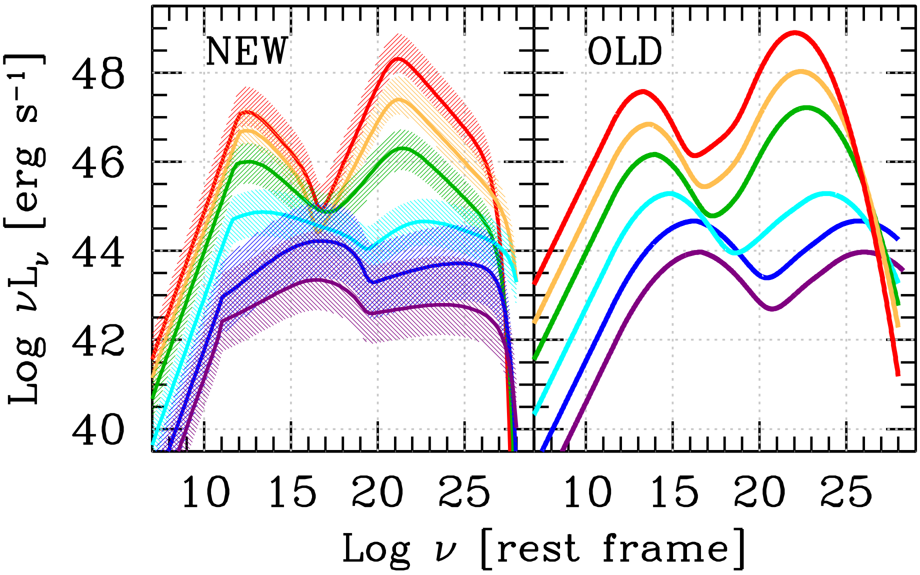

Figure 3: The blazar sequence: on the right the original version [30], based on bins of radio luminosity. On the left, the new version “2.0" based on bins of gamma-ray luminosity and using *Fermi* data. From ref. [31].

latter case the object is then called “extreme BL Lac" [28].

This sequence of SEDs is mirrored in the gamma-ray band, as traced by the spectrum measured with the *Fermi*-LAT detector [29]: albeit with a wide scatter, the gamma-ray slope smoothly shifts from steep (photon index $\Gamma > 2$) to hard ($\Gamma < 2$) as the sources transit from LSP to HSP-type SEDs (see Fig. 2, from [25]).

3. The *Fermi* blazar sequence

With the first all-sky survey in gamma-rays provided by EGRET, it was soon evident that there was a connection between the main blazars properties (SED type, bolometric and disk/lines luminosities). FSRQ are mostly of the LSP-type (only a few are ISP), they are the most luminous and display the largest Compton dominance (CD, i.e. the ratio of the gamma-ray to synchrotron peak luminosities/fluxes, $L_{IC}/L_{synch} \gtrsim 100$). BL Lacs instead span the widest range of SED types, from LSP to HSP to extreme BL Lacs, but tend to have more similar luminosities in the two peaks (except during flares). Binning sources in radio luminosity, used as proxy for the bolometric luminosity, a general trend emerged which was called “blazar sequence" [30, 32]: increasing the observed (i.e. beamed) total luminosity, the frequency of both peaks shifts to smaller values, while both the Compton dominance and the disk/line luminosity increase. Conversely, the highest SED peak frequencies were reached in the lowest-luminosity sources, with low Compton dominance and low/absent disk and emission lines.

This blazar sequence “v1.0" [30] was based on the available flux-limited samples in radio and X-rays, but the gamma-ray sampling was sparse (only 33 of the 126 objects considered were detected by EGRET), and inevitably biased towards the brightest sources/states due to the limited EGRET sensitivity. It therefore overestimated the gamma-ray contribution. With the advent of *Fermi*, a factor of $\sim 20\times$ in sensitivity was gained. It has thus become possible to revisit these

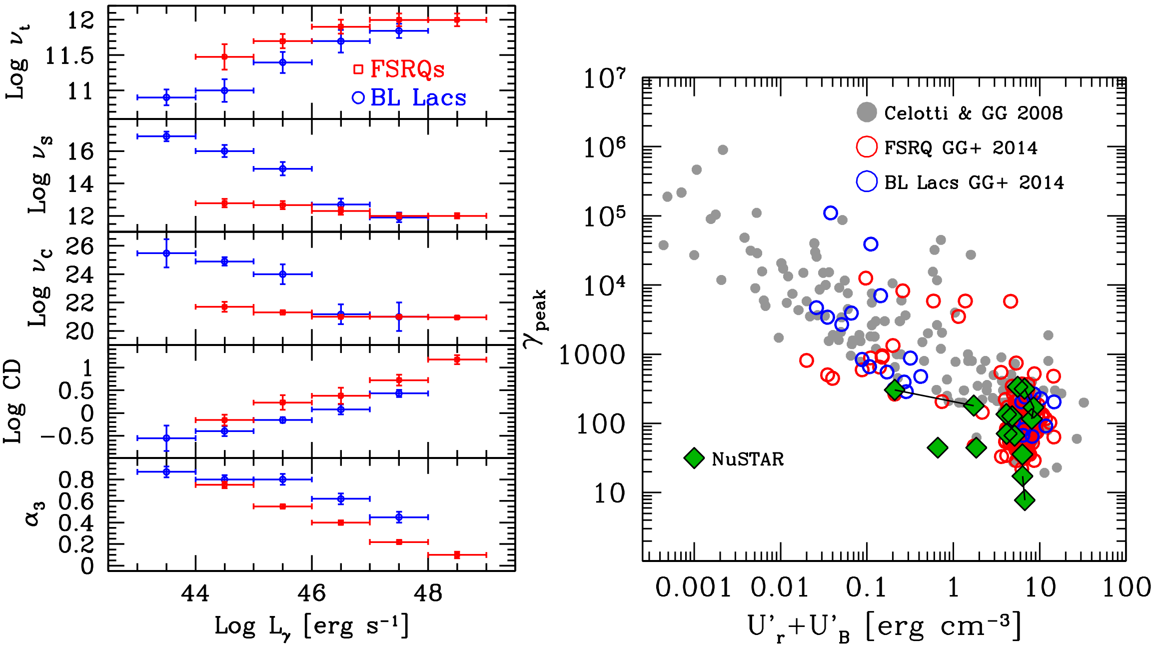

Figure 4: **Left**: main trends of the blazar sequence v2.0: note that for both FSRQ and BL Lacs the Compton dominance (CD) increases with luminosity, while only for BL Lacs both synchotron and Compton peaks (at ν_S and ν_C) shift to smaller frequencies as luminosity increases. Note also that, in FSRQ, the observed ν_S becomes comparable to the self-absorption frequency ν_t at high luminosity. From ref. [31]. **Right:** the random Lorentz factor γ_{peak} of the electrons emitting at the SED peak as a function of the total (radiative + magnetic) comoving energy density, from leptonic SSC+EC model fits. NuSTAR sources are powerful FSRQ at $z > 2$ observed with NuSTAR. From ref. [13].

trends on a much larger sample (considering 747 blazars with redshift from the clean 3LAC sample [25]) and using directly the gamma-ray luminosity as binning parameter, which provides a better proxy for the bolometric luminosity of a blazar due to its dominance in several objects. This constitute the “blazar sequence 2.0" [31]. The main outcome of this study is shown in Figure 3 and 4: the general trend is still confirmed, but with an important difference between FSRQ and BL Lacs. FSRQ have both peak energies which stay nearly constant as the luminosity changes, while BL Lacs shifts their peak frequencies. On the other hand, for both types the Compton dominance strongly increases with total power. In other words, the blazar sequence seems more a “BL Lac sequence" rather than for all blazars. Note however that the synchrotron self-absorption frequency ν_t increases with L_S (Fig. 4), and in the last 2 highest luminosity bins for FSRQ it becomes of the same order of the synchrotron peak frequency ($\nu_S \sim \nu_t \sim 10^{12}$ Hz). Therefore, what we observe as synchrotron peak frequency might be instead ν_t, since the flux emitted at ν_S can be self-absorbed. This might be part of the reason why FSRQ do not seem to shift their peak.

Both versions of the blazar sequence are interpreted as due to a different balance between acceleration and cooling of electrons [32, 33, 31]: more powerful objects with luminous disks and broad lines tend to have stronger cooling (by both synchrotron and inverse Compton on the relativistically amplified external photon fields), and thus have an SED which peaks at lower energies (LSP-type) and with higher Compton dominance. When radiative cooling is less (because of lower jet luminosity, lower magnetic field and absence of external radiation fields), the balance is reached progressively at higher energies and so the peaks shifts to higher frequencies (HSP-type SED). Indeed, fitting all SEDs with a leptonic model, the resulting Lorentz factor γ_{peak} of the electrons emitting at the peak is anti-correlated with the total magnetic plus radiative comoving energy density (see Fig. 4). This scenario agrees well with the different FSRQ/BL Lac behaviour: in FSRQ cooling is dominated by the external field (from BLR and/or molecular torus). Since both structures scale as $R \propto L_{disk}^{1/2}$, the energy density inside them (which is $\propto L_{disk}/R^2$) stays roughly constant, and thus their cooling rate. In true BL Lacs instead, the radiative energy density varies with luminosity.

On the other hand, the blazar sequence (which is an observed trend) might not be real. It is still strongly debated if it is indeed an intrinsic physical property of the blazar population or it is just the result of selection biases, given that a significant fraction of the BL Lac population is still missing redshift measurements (see e.g. ref [34]). Indeed it was demonstrated that a common asymmetric distribution of γ_{peak} peaked at $\sim 10^3$ but with no correlation with luminosity, together with minimal assumptions and a luminosity function for all blazars $\propto L^{-3}$ could reproduce the observed data just by selection biases, with no blazar sequence [34]. This alternative view seems to predict a very large number of low-power LSP BL Lacs, which should have a peak by SSC in the 1-10 keV range [33]. Future data from *eROSITA* might provide an answer in this respect [35].

The issue is still open, nevertheless some points are worth noting:

1) Compton dominance plays a crucial role in the blazar sequence, since its inception: without the higher luminosity in the gamma-ray peak, the correlation SED vs total luminosity was not significant enough already in the original sequence (see [30]). The real correlation is actually between the Compton dominance and the SED peak frequency: this is confirmed even more firmly with *Fermi* [36].

2) On the other hand, *Fermi* has unveiled several FSRQ and BL Lacs with low power and LSP-type SED, with low Compton dominance. Conversely, there is still no evidence for high-power HSP-type of SED (except the trend during short flares).

3) The existence of several low-power low-CD FSRQ seem to go against the idea of external Compton as main emission mechanism in these objects. On the other hand, the external-photons energy density seen in the jet comoving frame is strongly dependent on the bulk Lorents factor Γ (since it is amplified by Γ^2). Thus a slightly lower speed could accomodate these low-CD FSRQ.

4) If indeed FSRQ are dominated by external Compton on BLR photons, this should translate to a clear cut-off in the GeV spectrum due to γ-γ collisions with the same BLR photons. This seems not the case, as shown in the following section.

4. No BLR photons for jet electrons

The EC mechanism on UV photons from the BLR has been so far the most common scenario to model the SED of gamma-ray detected FSRQ (e.g. [32, 16, 33, 36]). It provides a straightforward way to explain both the difference in SED between FSRQ and BLLac objects and the observed fast variability (few days to hours), indicative of compact emitting regions. However, those same external photons become targets for the γ-γ collision and pair production process. The energy densities U_{rad} obtained from the BLR-size/luminosity relation given by reverberation mapping ($R_{\rm BLR} \sim 10^{17} L_{disk,45}^{1/2}$cm), and used in EC models [16, 17, 37], are large, of the order of $\sim$0.01

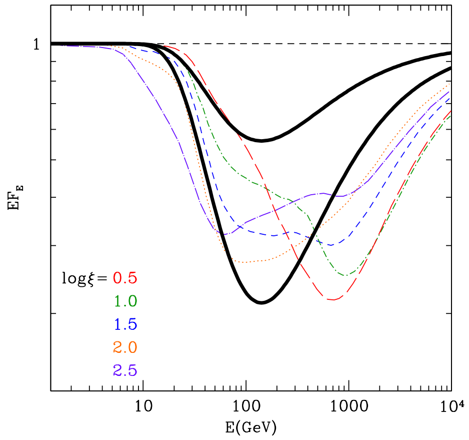

Figure 5: Comparison of the photon spectrum transmitted through the BLR radiation field computed with the spectral synthesis code XSTAR (at different ionization levels ξ but same total column density, colored lines, from ref. [44]) and with the black body approximation peaked at 10.2 eV (full black lines). The approximation is very good in the range of the cut-off region relevant for the LAT spectra, i.e. 10-100 GeV, for most ionization levels ξ. The incident spectrum (dashed black line) is taken as a power-law of photon index $\Gamma = 2$.

erg cm^{-3}. The resulting optical depth τ becomes huge on photon paths as short as 10^{16} cm. Thus a strong cut-off is expected in the gamma-ray spectrum of EC-dominated FSRQ, appearing above $\sim$20 GeV rest-frame and with maximum absorption at $\sim$100-200 GeV, (corresponding to the peak of the γ-γ cross section). Yet some FSRQ have already been detected at very high energies (VHE, $\gtrsim$100 GeV), indicating an emission outside the BLR [38, 39, 40, 41, 42]. So far such cases were considered occasional events, while the majority of the dissipation events was still expected to take place inside the BLR.

Taking advantage of $\sim$7.3 years of exposure by *Fermi* and the new PASS8 analysis, we have recently tested this scenario on the spectra of the 100 brightest FSRQ detected by *Fermi*-LAT [43]. We used the same assumptions and values commonly adopted in the EC models for the same sources [16, 17]. The BLR spectrum was approximated with a Planckian spectrum peaked at 10.2 eV, renormalized to match the BLR energy density. This provides a good approximation to the optical depth curve from the Hydrogen Lyα emission and recombination continuum complex [44], over a wide range of ionization states (see Fig. 5).

The LAT spectrum was first fitted up to 13 GeV rest-frame (the unabsorbed part), with power-law and log-parabolic models, and then extrapolated at higher energies, fitting the optical depth $\tau(E) = \ell\,\tau_{16}(E)$ to the data (where $\tau_{16}(E)$ is the optical depth for a path of 10^{16} cm). We tested fits both fixing the spectral parameters to the best-fit values in the unabsorbed range, and with all parameters free to vary. The resulting photon path length ℓ and optical depth $\tau_{\rm max}$ are to be compared with the values obtained from inside the BLR, $\ell_{\rm BLR}$ and $\tau_{\rm max}^{\rm BLR}$. As benchmark, we assumed a dissipation region $R_{\rm diss}$ located at $R_{\rm BLR}/2$ (i.e. halfway between the BH and the BLR), with a lower limit of 2×10^{16} cm. Therefore $\tau_{\rm max}^{\rm BLR}$ is the optical depth corresponding to $\ell_{\rm BLR} = R_{\rm BLR} - R_{\rm diss}$.

Surprisingly, there is no evidence for the expected BLR cut-off, even in sources with large disk luminosities and BLR sizes (see Fig. 6). For 2/3 of the sample, the LAT data exclude any significant

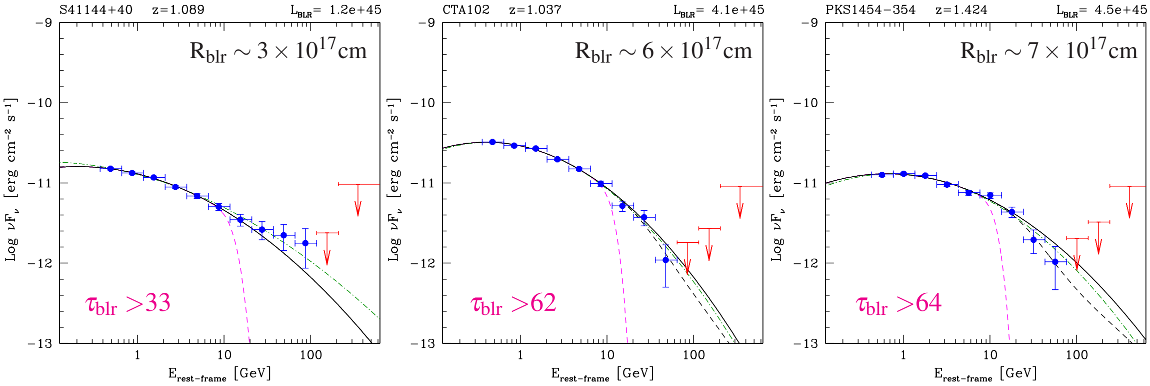

Figure 6: Test of the EC(BLR) model on the gamma-ray SED of 3 FSRQ characterized by a large disk luminosity and BLR size, as labelled. The spectra do not show evidence of important γ-γ absorption. Solid lines show the fit with parameters determined below 13 GeV rest-frame. Black dashed lines show the same spectrum fitted with free BLR absorption, magenta lines the same spectrum with the optical depth expected if $R_{\rm diss} = R_{\rm BLR}/2$, as labelled (see text). Dot-dashed green lines show the fit of a pure log-parabolic model to the whole spectrum, wihtout BLR absorption. From ref. [43].

absorption ($\tau_{\rm max} < 1$), while for the remaining 1/3 the possible absorption is constrained to be 1.5–2 orders of magnitude lower than expected (see Fig. 7).

This result holds considering the emission from either a localized region inside the BLR or a single relativistic blob traveling over the whole BLR size. In the latter case, the observed gamma-rays are produced at different distances inside the BLR, with decreasing optical depth (since the photon path inside the BLR is progressively shorter). As a result, the time-integrated spectrum does not appear attenuated by $e^{-\tau(E,\ell)}$ as before, but has a shallower shape which goes as τ^{-1} for large values of τ [43]. Even considering this scenario, the limits on the path length increase only mildly, by a factor 2-3. The large majority of objects still do not show significant absorption (see Fig. 7, magenta histogram). This result holds also dividing the spectra in high and low-flux states, for the 20 brightest sources with enough statistics, and for powerful blazars with the largest BLR. Only 1 object out of 10 seems compatible with substantial attenuation ($\tau_{\rm max} > 5$).

The inevitable conclusion is that for 9 out of 10 Fermi blazars of FSRQ type, *the jet does not interact with BLR photons*, for most of the time or most of the flux, contrary to the EC model's assumption.

4.1 Alternatives ?

To keep τ low inside the BLR, two straightforward possibilities are: 1) to decrease the photon densities by enlarging the size of the BLR (e.g. if the radius from reverberation mapping is actually underestimated), and 2) to shift the γ-γ threshold at higher energies by selecting preferred angles of interaction (e.g. if the BLR is flattened along the accretion disk).

Both scenarios do not save the EC(BLR) model. In the first case, since $\tau \propto 1/R_{\rm BLR}$, a factor 100× lower in τ means that the size of the BLR should be 100× larger (in fact close to the torus size). This implies a factor 10^{-4} lower energy density for the BLR photons, which put them below all other available energy densities (e.g. by infrared photons or B). In the second case, to push the 20 GeV absorption cut-off outside the observed data (e.g. at least to 100 GeV rest-frame), an

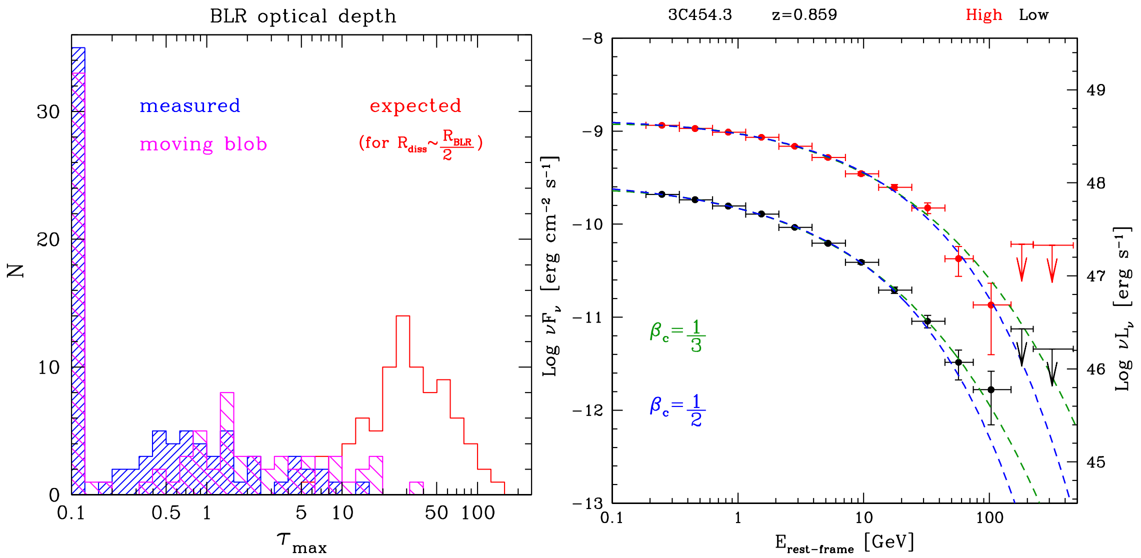

Figure 7: **Left:** histogram of the distribution of measured vs expected maximum optical depths τ_{max} (i.e. at the peak of the γ-γ cross-section), for the 83 objects with BLR luminosity estimates. Where $\tau_{max} \leq 0.1$, objects are counted in the first bin. Three emission scenario are considered: from deep inside the BLR, as in EC models (red histogram), from a fixed location inside the BLR (blue histogram) and from a moving-blog emitting up to the BLR radius (magenta histogram). The LAT data indicate that the maximum optical depth due to BLR photons is at most ∼30-100x *lower* than typically used in EC(BLR) models, and it is <1 in ∼2/3 of the sample. **Right:** spectra of 3C 454.3, in high and low state, fitted with a spectrum $N(E) \propto E^{-\Gamma} exp(-(E/E_C)^{\beta_c})$ with two different exponents β_c, corresponding to IC with synchrotron (1/3) or external Planckian photons (1/2). Details in text and refs. [43, 45].

average shift of $\sim 5\times$ of the energy threshold is required. Geometrical considerations show that the preferred angle should be <30 degrees, meaning that the region should already be outside the BLR radius. Both alternatives do not seem able to keep EC on UV BLR photons as a viable mechanism for the gamma-ray emission in FSRQ.

The main caveat is given by the long integration times, necessary given the small collection area of *Fermi*-LAT (~ 1 m^2). In principle, there is the possibility that a series of short hard flares occurring beyond the BLR might provide all the detected high-energy photons, while for most of the time the emission comes from inside the BLR. This could skew the fit simulating the effects of a lower absorption, in the averaging process. It seems unlikely because of the fine tuning required: flares should be frequent, short but not too strong in order to remain below the threshold of the high/low-state separation, and for nearly all sources in our sample.

4.2 Consequences

This result has two direct consequences. The first is that VHE gamma-rays are not suppressed by the BLR photons. Therefore most FSRQ –even 3C454.3– can be copious emitters of VHE gamma-rays under proper conditions, and could become easily detectable by Cherenkov telescopes especially during HBL-like flares (see next section).

The second consequence is that the spectral shape of the radiation at high energies is not determined by absorption, but by the end of the particle spectrum. This opens up new diagnostic possibilities because of a direct link between the electron distribution and the upscattered photons in the cut-off region [45]. An example is given by the spectra of 3C 454.3 (see Fig. 7). If the electron distribution is a power-law with an exponential cutoff of the form $exp(-(E/E_C)^2)$, as expected when the cooling is $\propto \gamma^2$, the Thomson-upscattered gamma-ray spectrum will have a shape $\propto E^{-\Gamma} exp(-(E/E_C)^{\beta_c})$ with a smoother, under-exponential cut-off as $\beta_c = 1/3$ or $1/2$ depending on the target radiation field, synchrotron or Planckian [45]. Indeed both shapes provide an excellent fit to the LAT data of 3C454.3, in both high and low states, with a slight statistical preference for a Planckian field in high state (maybe the IR photons from the molecular torus) and for SSC in low state. The comparison with the synchrotron spectrum could pin down the shape of the emitting particles at the highest energies (see also ref. [46])

This result does not clash with the interpretation of the blazar sequence, but it limits the origin of the external photons to the IR torus or other parts of the jet. However, all jet physical parameters derived from the SED modeling must change, depending on the emission mechanism and dominant seed photons, because the frequency of the external photons shifts from UV to IR. Given the strong correlation between gamma-ray luminosity and BLR emission in *Fermi* blazars [20], this result suggests that the BLR acts as a proxy for the accretion properties but does not affect directly the jet emission through cooling.

On the contrary, the absence of BLR interactions make more understandable another new phenomenology discovered by *Fermi*: namely the HSP-like flares in FSRQ.

5. HSP-like flares in LSP

On average, Fermi-LAT spectra of blazars follows the SED sequence as traced by the synchrotron peaks (see Fig. 2). However, in the last years several FSRQ and LSP sources have shown during flares hard LAT spectra which are typical of HSP sources, without apparently changing their LSP character in the synchrotron hump. If the radiative cooling were dominated by BLR photons, such high gamma-ray peak energies would not be easy to obtain, because of the very fast cooling expected. The much lower energy density of IR photons from the torus, instead, (or even a standard SSC mechanism) leaves more room to explain these states.

In absence of BLR absorption, the hard LAT spectra provide proof that FSRQ/LSP sources are capable of high VHE fluxes during such flares, even after the EBL attenuation, well within the sensitivity of present Cherenkov telescopes in just few hours [43]. Figure 8 shows four striking examples of these unexpected gamma-ray spectra in four famous objects: 3 FSRQ (among which the neutrino source TXS 0506+056, possibly an FSRQ in disguise [12]) and BL Lac itself.

The origin of these spectra is not yet clear: if it is a new component emerging only temporarily (sort of mini-HSP zone inside a main LSP-type outflow), one would expect it to appear in the X-ray band as well, by synchrotron, in the form of a steep X-ray spectrum of higher flux. This seems not the case, requiring a huge Compton dominance of the new component to stay consistent with the data. These HSP-like states have been reported so far only during active states, but that could be partly due to an observational bias.

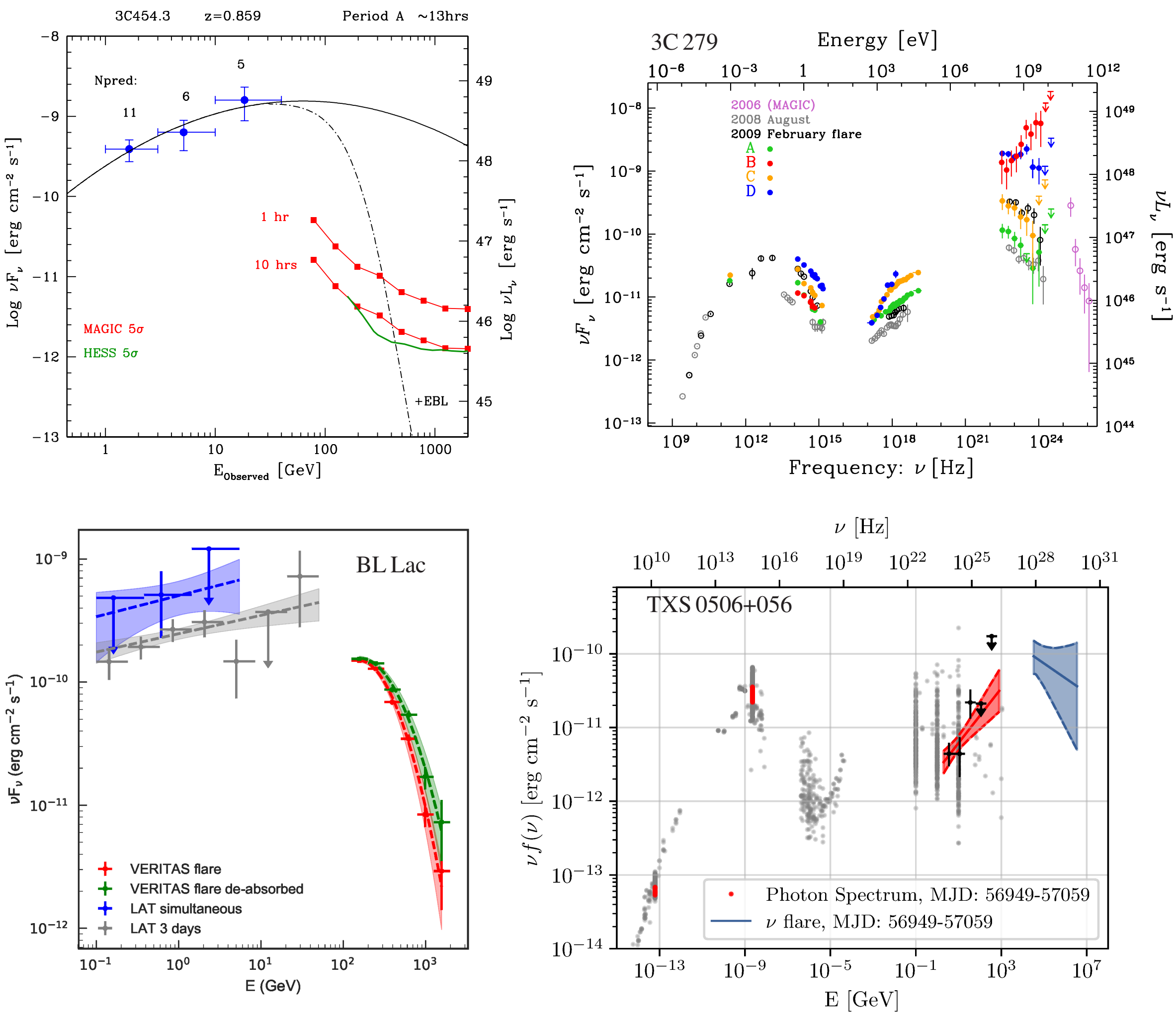

Figure 8: SED gamma-ray spectra of 4 LSP/ISP blazars of both FSRQ and BL Lac types, showing gamma-ray states typical of HSP sources. Integration times range from few hours to several days. The 3C 454.3 plot shows also the sensitivity curves of present Cherenkov telescopes. From refs. [43, 47, 48, 49].

6. Extreme-TeV BL Lacs

At the opposite end of the blazar sequence, extreme-TeV BL Lacs are a new type of HSP BL Lacs (HBL) characterized by a hard intrinsic VHE spectrum ($\Gamma_{\rm VHE} \lesssim 1.5 - 1.9$, see e.g. [50, 51, 52, 53, 54]), after correction for the effects of γ-γ interactions with the diffuse Extragalactic Background Light (EBL, see e.g. [55, 56, 57]). This locates their gamma-ray peak in the SED above 2-10 TeV (see Fig. 9), the highest peak energies ever seen in blazars and 1-2 orders of magnitude higher than regular HSP BL Lacs. A hard spectrum at such high energies is difficult to obtain by IC in blazars, using standard one-zone leptonic models for the whole SED. Both the decrease of the scattering efficiency in the Klein-Nishina regime and the lower energy density of the seed photons available for scatterings in the Thomson regime, as the gamma-ray energy increases, tend to steepen the TeV spectrum.

So far, extreme-TeV BL Lacs seem to constitute about 1/4 of all HBLs detected at VHE [58]. By synchrotron, most (but not all) of them are also of the extreme type, i.e. with the synchrotron

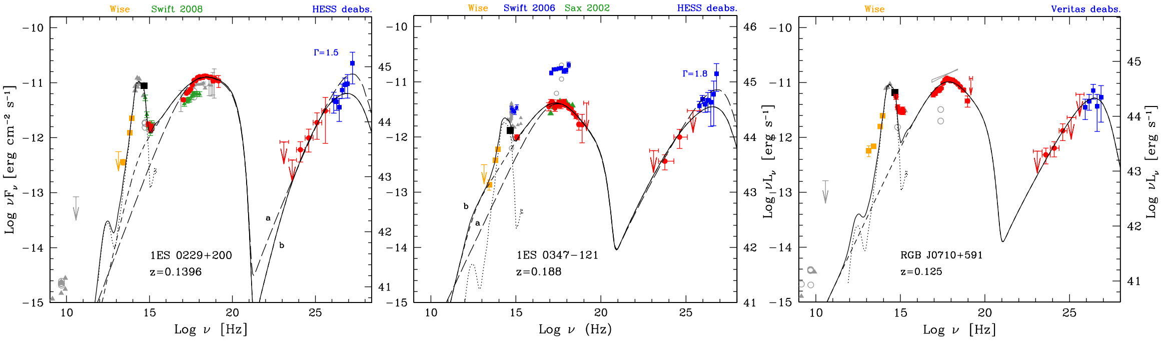

Figure 9: SEDs of 3 extreme-TeV BL Lacs, with new simultaneous Swift-NuSTAR-Fermi data shown in red. Historical data taken approximately in the same epoch of the VHE data are shown in blue. The VHE data are corrected for EBL absorption following [59]. Solid lines show the sum of the theoretical SSC model (short-dashed line) and host-galaxy emission (dotted line). From ref. [54].

peak above 1 keV up to 100 keV and beyond.

Hard TeV spectra could be the result of a new narrow-peaked electron population, whose synchrotron emission should be visible in hard X-rays. However this seems excluded by recent NuSTAR-Swift observations, which pinned down the spectrum of the synchrotron hump for six objects, from UV to hard X-rays [54]. A one-zone SSC model can in principle reproduce the extreme properties of both peaks in the SED, from X-ray up to TeV energies. However, it requires 1) peak electrons of very high energy (random Lorentz factors $\gamma \gtrsim 10^6$) with extremely low radiative efficiency, 2) milliGauss magnetic fields and conditions heavily out of equipartition (by 3 to 5 orders of magnitude), and 3) to give up the requirement to fit the UV data, which then should belong to a different emission component [54]. There is indeed evidence in two objects of a separation between the UV and X-ray emission (see Fig. 9), with the extrapolation of the X-ray power-law spectrum at lower energies falling below the UV flux.

Whatever scenario is considered, radiative cooling must be strongly inhibited: the TeV electrons cannot “see” UV or lower-energy photons, even if coming from different zones/populations, otherwise the increased radiative cooling in Thomson regime would steepen the VHE spectrum. This implies that even the assumption of a structured jet –namely a fast spine surrounded by a slower layer– would not help in reaching equipartition [54].

Conditions so far away from equipartition are puzzling also because not limited to a flaring episode: the extreme-TeV spectra in most of these BL Lacs seem to last for years. There must be a mechanism which keep the conditions persistently out of equipartition. The high values of the ratio of particles to magnetic field energy density ($U_{\rm e}/U_{\rm B} \sim 10^3 - 10^5$) seems also to exclude magnetic reconnection as acceleration mechanism. Models predict an upper limit of the order of $U_{\rm e}/U_{\rm B} \sim 3$ in the dissipation region [60]. These blazars might be revealing something new about the processes at work in relativistic jets.

6.1 How to find them ?

So far only a handful of these extreme-TeV sources have been identified. Part of the reason is that they can be identified only through VHE observations, requiring dedicated campaigns by atmospheric Cherenkov telescopes arrays, which can be done on few targets per year.

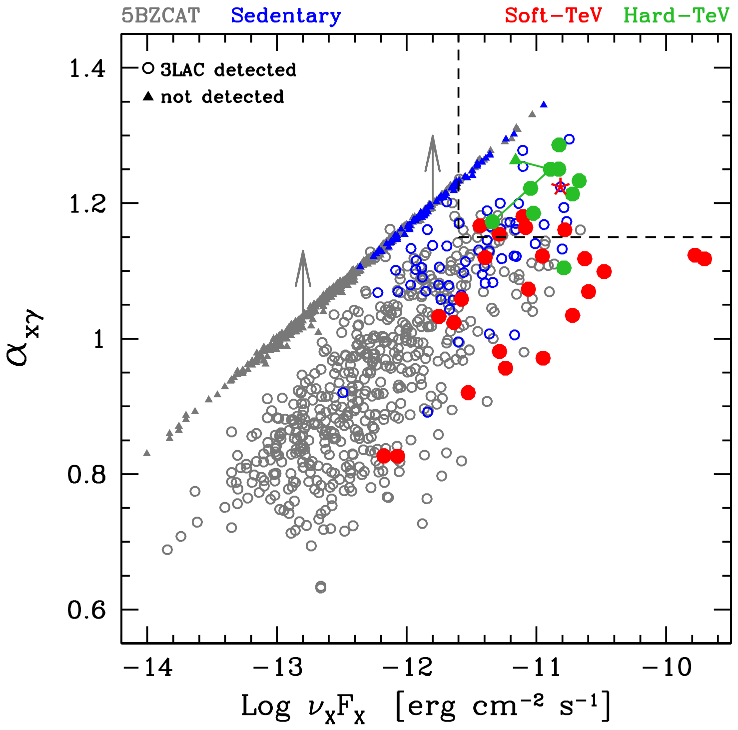

Figure 10: plane of the broad-band index $\alpha_{x\gamma}$ vs the X-ray νF_ν flux at 1 KeV, for all BL Lacs in the Sedentary Survey and 5BZCAT samples (blue and grey markers, respectively). Gamma-ray data are obtained from the Fermi 3LAC catalog (open circles). For non-detected objects (triangles), a reference flux of 8e-11 cm^{-2} s^{-1} (in the 1-100 GeV band) is adopted as upper limit. This translates to a lower limit to $\alpha_{x\gamma}$, as indicated by the arrows. Given the correlation between the axes, the non-detected objects form a line in the figure (whose scatter is given by the K-correction). The red star marks the position of 1ES 1426+428, which is extreme in synchrotron but not in TeV. The green lines connect the positions of the prototypical hard-TeV BL Lac 1ES 0229+200 in 3 different states: 1) during the first 2 years of *Fermi* operation (upper limit from the 2LAC catalog with same-epoch Swift data); 2) detection in years 2011-2013 with average RXTE flux in the same epoch; 3) 3LAC catalog values as the other objects. From ref [58].

To narrow down the potential candidates, a pre-selection is necessary. So far, the selection criteria for BL Lacs have been generally aimed at TeV-emitting sources (i.e. at maximizing the VHE flux). They might not work for extreme-TeV sources, and in fact they are biased *against* them. When the gamma-ray peak is in the 10-300 GeV range, as for standard HBL with soft-TeV spectra, a blazar tends to be bright and easily detectable in *Fermi* as well as VHE, because both bands are close to the maximum of the emission. Hard-TeV BL Lacs instead have generally a much lower flux in *Fermi* than regular (soft-TeV) BL Lacs, at similar SED luminosities. This because, as the gamma-ray peak shifts towards multi-TeV energies, the LAT band falls more and more inside the valley between synchrotron and Compton humps, where the emission is much fainter.

Somewhat counter-intuitively, therefore, the extreme-TeV candidates should be looked for among blazars with the *lowest* –not the highest– gamma-ray flux in *Fermi*, for a given synchrotron flux. The latter is traced by the X-ray flux around 1 keV, which is close to the peak of the synchrotron emission in HBL. Thus the most promising extreme-TeV candidates should be those with the largest X-ray to GeV flux ratio, i.e. with the highest broad-band index $\alpha_{x\gamma}$.

Figure 10 shows $\alpha_{x\gamma}$ as a function of the X-ray flux, for a large sample of BL Lacs [58]. Indeed the known hard-TeV BL Lacs cluster in the region of high $\alpha_{x\gamma}$ and high X-ray flux. The region determined by the location of the known extreme-TeV objects can thus be considered a good criterium for the selection of new TeV-peaked candidates [58].

7. Ultra-fast variability

Ultra-fast variability is another new and surprising behaviour of relativistic jets discovered in the last decade, as soon as large-area gamma-ray detectors became operational. It is defined when the observed variability time becomes comparable or less than the light-crossing time of the putative Black Hole (e.g. $\tau_0 \equiv R_S/c$). It is surprising because it apparently defies the paradigm that the minimum variability in the jet is imprinted by the scale of the central BH horizon (relativistic beaming cannot shorten the variability timescale imprinted by a source that is stationary in the observer's frame, as pointed out by ref [61]). It thus indicates that the observed variability is determined either by a fraction of the BH horizon, or by small-scale fluctuations intrinsic to the jet itself [61]. The most striking example is provided by the huge flare of PKS 2155-304, with doubling timescales < 2 minutes corresponding to $\sim 0.01\tau_0$ but yielding a flux 10-100× higher than the everyday whole source luminosity [62].

Possible mechanisms to obtain such variability are a region that move relativistically in the jet frame which in turn moves relativistically toward the observer (e.g. jet-in-jet models [63, 64]), or a perturbation imprinted on the jet from outside, on scales much smaller than the gravitational radius (e.g. the jet-meets-star scenario, [65]), or produced directly in the BH magnetosphere [66, 67]. See ref [68] for a full discussion.

Here I want to point out that such phenomenon is now observed in almost every type of jetted AGNs. It is observed in every class of blazars, be it BL Lacs of HSP type as PKS 2155-304 [62] and Mkn 501 [69] or LSP-type as BL Lac itself [48], or FSRQ as 3C 279 in 2015 [47], PKS 1510-089 [70] and 4C 21.35 [71] (the latter at VHE, indicating an extremely compact region outside the BLR). It is also observed in slightly misaligned jets, like the radiogalaxies M87 [72, 73] and IC 310 [74, 75]. In the latter case, a luminosity higher than the upper limit of 2×10^{43} erg s^{-1} for 5-minute flares seems to exclude a BH magnetosphere origin of the flare detected from IC 310 [76].

8. Superluminal motion in HSP

One of the long-standing problems in blazar physics is the apparent discrepancy between the high bulk-motion Lorentz factors required by gamma-ray transparency and SED modeling ($\Gamma \sim 20-50$) and the absence of significant superluminal motion at the VLBI scale (so-called “bulk Lorentz factor crisis"). While FSRQ and LSP-type blazars show high apparent jet speed, up to 30-40, the VLBI radio knots seem stationary or at most subluminal in HSP-type BL Lacs [77]. This is particularly evident in Mkn 421, for example on the results of the MOJAVE survey [78]. Absence of superluminal motion is expected for very small viewing angles, but that hypothesis would make the parent population numbers larger than the known radio-loud population.

So far it has been generally assumed that the jet was partially disrupted or stopped before the VLBI scale, and/or that the VLBI knots were the location of standing recollimation shocks accelerating particles along the jet. Evidence for the latter is now emerging from 13 years of observations with Swift [78]. Stacking the X-ray lightcurves of 6 different active periods in Mkn 421, a common variability pattern seems to emerge. It is consistent with a main flare emission zone located in the most upstream 15.3 GHz radio knot, at 0.38 mas from the core. Subsequent peaks in the lightcurve are then consistent with a perturbation crossing all the downstream radio knots with a constant apparent speed $\beta = 45c$ [78].

This seems to confirm that the jet is indeed highly relativistic at the VLBI scale also in HSP blazars, but it also confirms that the dissipation zones along the jet are much more stationary at certain distances from the BH than in FSRQ, denoting another essential difference in jet structure between these two blazar classes.

9. Concluding remarks

Despite the amount of new sources and data provided by *Fermi*-LAT and Cherenkov telescopes, and the confirmation of some general trends, new phenomena are undermining our basic assumptions in blazar modeling. Until a consistent explanation is found, our understanding of blazars has become somewhat fuzzier than before (and for this more interesting!).

The gamma-ray data are showing that BLR photons are not the main seed photons for the IC mechanism, undermining the main explanation of the difference in SED properties between FSRQ and BL Lacs. The alternative for the EC mechanism is given by the IR photons from the torus [79, 17], though this implies a change of the derived jet parameters.

The discovery of extreme-TeV BL Lacs is challenging also the SSC paradigm. The parameters for it to work look somewhat unrealistic (mG magnetic fields, pile-up electrons distributions, steadily out of equipartition by 5 orders of magnitude) and the necessity of multiple ad-hoc components to explain the SED kills the elegance and simplicity of the original concept. The gamma-ray emission in these sources might in fact be produced by a different process.

Neutrino production and ultrafast variability remain a puzzle, as well as the particle acceleration rate, which even in the most extreme cases seems orders of magnitude less than in the Crab or SNRs.

Beside the upcoming *eROSITA* and CTA telescopes, polarization measurements in X-rays might soon provide new precious insights for the emission scenarios. The upcoming *Imaging X-ray Polarimetry Explorer* (IXPE, [80]) will both study the synchrotron radiation in HSP sources and test the inverse Compton emission in LSP sources. For the latter, because inverse-Compton scattering by relativistic electrons reduces the degree of polarization of a polarized target photon field by at least ~1/2 (e.g. [81]), the detection of a high level of polarization might indicate a synchrotron origin of the second hump, requiring a deep revision of the blazars standard picture.

Acknowledgments

I wish to thank the organizers for their kind invitation to give this review talk, and for the usual excellent hospitality.

References

[1] S. Rawlings and R. Saunders, *Evidence for a common central-engine mechanism in all extragalactic radio sources*, Nature **349** (1991) 138.

[2] A. Celotti and G. Ghisellini, *The power of blazar jets*, MNRAS **385** (2008) 283 [0711.4112].

[3] Event Horizon Telescope Collaboration, K. Akiyama, A. Alberdi, W. Alef, K. Asada, R. Azulay et al., *First M87 Event Horizon Telescope Results. I. The Shadow of the Supermassive Black Hole*, ApJ **875** (2019) L1 [1906.11238].

[4] M. Sikora and G. Madejski, *On Pair Content and Variability of Subparsec Jets in Quasars*, ApJ **534** (2000) 109 [astro-ph/9912335].

[5] G. Ghisellini and F. Tavecchio, *Compton rockets and the minimum power of relativistic jets*, MNRAS **409** (2010) L79 [1008.1982].

[6] G. Ghisellini, F. Tavecchio, L. Maraschi, A. Celotti and T. Sbarrato, *The power of relativistic jets is larger than the luminosity of their accretion disks*, Nature **515** (2014) 376 [1411.5368].

[7] R. Narayan, Y. Zhu, D. Psaltis and A. SaĬe11owski, *HEROIC: 3D general relativistic radiative post-processor with comptonization for black hole accretion discs*, MNRAS **457** (2016) 608 [1510.04208].

[8] A. Tchekhovskoy, R. Narayan and J. C. McKinney, *Efficient generation of jets from magnetically arrested accretion on a rapidly spinning black hole*, MNRAS **418** (2011) L79 [1108.0412].

[9] IceCube Collaboration, M. G. Aartsen, M. Ackermann, J. Adams, J. A. Aguilar, M. Ahlers et al., *Multimessenger observations of a flaring blazar coincident with high-energy neutrino IceCube-170922A*, *Science* **361** (2018) eaat1378 [1807.08816].

[10] IceCube Collaboration, M. G. Aartsen, M. Ackermann, J. Adams, J. A. Aguilar, M. Ahlers et al., *Neutrino emission from the direction of the blazar TXS 0506+056 prior to the IceCube-170922A alert*, *Science* **361** (2018) 147 [1807.08794].

[11] F. Halzen, *Cosmic Neutrinos and the Cosmic-Ray Accelerator TXS 0506+056*, *arXiv e-prints* (2019) arXiv:1909.09468 [1909.09468].

[12] P. Padovani, F. Oikonomou, M. Petropoulou, P. Giommi and E. Resconi, *TXS 0506+056, the first cosmic neutrino source, is not a BL Lac*, MNRAS **484** (2019) L104 [1901.06998].

[13] G. Ghisellini, M. Perri, L. Costamante, G. Tagliaferri, T. Sbarrato, S. Campitiello et al., *A NuSTAR view of powerful γ-ray loud blazars*, A&A **627** (2019) A72 [1906.02955].

[14] G. Tagliaferri, G. Ghisellini, P. Giommi, L. Chiappetti, L. Maraschi, A. Celotti et al., *The concave X-ray spectrum of the blazar ON 231: the signature of intermediate BL Lacertae objects*, A&A **354** (2000) 431 [astro-ph/9912055].

[15] H. Krawczynski, S. B. Hughes, D. Horan, F. Aharonian, M. F. Aller, H. Aller et al., *Multiwavelength Observations of Strong Flares from the TeV Blazar 1ES 1959+650*, ApJ **601** (2004) 151 [astro-ph/0310158].

[16] G. Ghisellini and F. Tavecchio, *Canonical high-power blazars*, MNRAS **397** (2009) 985 [0902.0793].

[17] M. Sikora, Ł. Stawarz, R. Moderski, K. Nalewajko and G. M. Madejski, *Constraining Emission Models of Luminous Blazar Sources*, ApJ **704** (2009) 38 [0904.1414].

[18] C. M. Urry and P. Padovani, *Unified Schemes for Radio-Loud Active Galactic Nuclei*, PASP **107** (1995) 803 [`astro-ph/9506063`].

[19] P. Giommi, P. Padovani and G. Polenta, *A simplified view of blazars: the γ-ray case*, MNRAS **431** (2013) 1914 [`1302.4331`].

[20] T. Sbarrato, P. Padovani and G. Ghisellini, *The jet-disc connection in AGN*, MNRAS **445** (2014) 81 [`1405.4865`].

[21] N. I. Shakura and R. A. Sunyaev, *Reprint of 1973A&A....24..337S. Black holes in binary systems. Observational appearance.*, A&A **500** (1973) 33.

[22] R. Narayan and I. Yi, *Advection-dominated Accretion: Underfed Black Holes and Neutron Stars*, ApJ **452** (1995) 710 [`astro-ph/9411059`].

[23] G. Ghisellini, F. Tavecchio, L. Foschini and G. Ghirland a, *The transition between BL Lac objects and flat spectrum radio quasars*, MNRAS **414** (2011) 2674 [`1012.0308`].

[24] P. Padovani, *Active Galactic Nuclei at all wavelengths and from all angles*, *Frontiers in Astronomy and Space Sciences* **4** (2017) 35.

[25] M. Ackermann, M. Ajello, W. B. Atwood, L. Baldini, J. Ballet, G. Barbiellini et al., *The Third Catalog of Active Galactic Nuclei Detected by the Fermi Large Area Telescope*, ApJ **810** (2015) 14 [`1501.06054`].

[26] P. Padovani and P. Giommi, *The connection between x-ray- and radio-selected BL Lacertae objects*, ApJ **444** (1995) 567 [`astro-ph/9412073`].

[27] G. Calderone, G. Ghisellini, M. Colpi and M. Dotti, *Black hole mass estimate for a sample of radio-loud narrow-line Seyfert 1 galaxies*, MNRAS **431** (2013) 210 [`1212.1181`].

[28] L. Costamante, G. Ghisellini, P. Giommi, G. Tagliaferri, A. Celotti, M. Chiaberge et al., *Extreme synchrotron BL Lac objects. Stretching the blazar sequence*, A&A **371** (2001) 512 [`astro-ph/0103343`].

[29] W. B. Atwood, A. A. Abdo, M. Ackermann, W. Althouse, B. Anderson, M. Axelsson et al., *The Large Area Telescope on the Fermi Gamma-Ray Space Telescope Mission*, ApJ **697** (2009) 1071 [`0902.1089`].

[30] G. Fossati, L. Maraschi, A. Celotti, A. Comastri and G. Ghisellini, *A unifying view of the spectral energy distributions of blazars*, MNRAS **299** (1998) 433 [`astro-ph/9804103`].

[31] G. Ghisellini, C. Righi, L. Costamante and F. Tavecchio, *The Fermi blazar sequence*, MNRAS **469** (2017) 255 [`1702.02571`].

[32] G. Ghisellini, A. Celotti, G. Fossati, L. Maraschi and A. Comastri, *A theoretical unifying scheme for gamma-ray bright blazars*, MNRAS **301** (1998) 451 [`astro-ph/9807317`].

[33] G. Ghisellini and F. Tavecchio, *The blazar sequence: a new perspective*, MNRAS **387** (2008) 1669 [`0802.1918`].

[34] P. Giommi, P. Padovani, G. Polenta, S. Turriziani, V. D'Elia and S. Piranomonte, *A simplified view of blazars: clearing the fog around long-standing selection effects*, MNRAS **420** (2012) 2899 [`1110.4706`].

[35] A. Merloni, P. Predehl, W. Becker, H. Böhringer, T. Boller, H. Brunner et al., *eROSITA Science Book: Mapping the Structure of the Energetic Universe*, *ArXiv e-prints* (2012) [`1209.3114`].

[36] J. D. Finke, *Compton Dominance and the Blazar Sequence*, ApJ **763** (2013) 134 [`1212.0869`].

[37] G. Ghisellini and F. Tavecchio, *Fermi/LAT broad emission line blazars*, MNRAS **448** (2015) 1060 [`1501.03504`].

[38] J. Aleksić, L. A. Antonelli, P. Antoranz, M. Backes, J. A. Barrio, D. Bastieri et al., *MAGIC Observations and multiwavelength properties of the quasar 3C 279 in 2007 and 2009*, A&A **530** (2011) A4 [`1101.2522`].

[39] J. Aleksić, S. Ansoldi, L. A. Antonelli, P. Antoranz, A. Babic, P. Bangale et al., *MAGIC observations and multifrequency properties of the flat spectrum radio quasar <ASTROBJ>3C 279</ASTROBJ> in 2011*, A&A **567** (2014) A41 [`1311.2833`].

[40] J. Aleksić, L. A. Antonelli, P. Antoranz, M. Backes, J. A. Barrio, D. Bastieri et al., *MAGIC Discovery of Very High Energy Emission from the FSRQ PKS 1222+21*, ApJ **730** (2011) L8 [`1101.4645`].

[41] F. Tavecchio, J. Becerra-Gonzalez, G. Ghisellini, A. Stamerra, G. Bonnoli, L. Foschini et al., *On the origin of the γ-ray emission from the flaring blazar PKS 1222+216*, A&A **534** (2011) A86 [`1104.0048`].

[42] A. Abramowski, F. Acero, F. Aharonian, A. G. Akhperjanian, G. Anton, S. Balenderan et al., *H.E.S.S. discovery of VHE γ-rays from the quasar PKS 1510-089*, A&A **554** (2013) A107 [`1304.8071`].

[43] L. Costamante, S. Cutini, G. Tosti, E. Antolini and A. Tramacere, *On the origin of gamma-rays in Fermi blazars: beyondthe broad-line region*, MNRAS **477** (2018) 4749 [`1804.02408`].

[44] B. E. Stern and J. Poutanen, *The Mystery of Spectral Breaks: Lyman Continuum Absorption by Photon-Photon Pair Production in the Fermi GeV Spectra of Bright Blazars*, ApJ **794** (2014) 8 [`1408.0793`].

[45] E. Lefa, S. R. Kelner and F. A. Aharonian, *On the Spectral Shape of Radiation due to Inverse Compton Scattering Close to the Maximum Cutoff*, ApJ **753** (2012) 176 [`1205.2929`].

[46] C. Romoli, A. M. Taylor and F. Aharonian, *Cut-off characterisation of energy spectra of bright fermi sources: Current instrument limits and future possibilities*, *Astroparticle Physics* **88** (2017) 38 [`1608.01501`].

[47] M. Hayashida, K. Nalewajko, G. M. Madejski, M. Sikora, R. Itoh, M. Ajello et al., *Rapid Variability of Blazar 3C 279 during Flaring States in 2013-2014 with Joint Fermi-LAT, NuSTAR, Swift, and Ground-Based Multiwavelength Observations*, ApJ **807** (2015) 79 [`1502.04699`].

[48] A. U. Abeysekara, W. Benbow, R. Bird, T. Brantseg, R. Brose, M. Buchovecky et al., *Multiwavelength Observations of the Blazar BL Lacertae: A New Fast TeV Gamma-Ray Flare*, ApJ **856** (2018) 95 [`1802.10113`].

[49] P. Padovani, P. Giommi, E. Resconi, T. Glauch, B. Arsioli, N. Sahakyan et al., *Dissecting the region around IceCube-170922A: the blazar TXS 0506+056 as the first cosmic neutrino source*, MNRAS **480** (2018) 192 [`1807.04461`].

[50] F. Aharonian, A. G. Akhperjanian, A. R. Bazer-Bachi, M. Beilicke, W. Benbow, D. Berge et al., *A low level of extragalactic background light as revealed by γ-rays from blazars*, Nature **440** (2006) 1018 [`astro-ph/0508073`].

[51] F. Aharonian, A. G. Akhperjanian, U. Barres de Almeida, A. R. Bazer-Bachi, B. Behera, M. Beilicke et al., *New constraints on the mid-IR EBL from the HESS discovery of VHE γ-rays from 1ES 0229+200*, A&A **475** (2007) L9 [`0709.4584`].

[52] F. Tavecchio, G. Ghisellini, G. Bonnoli and L. Foschini, *Extreme TeV blazars and the intergalactic magnetic field*, MNRAS **414** (2011) 3566 [`1009.1048`].

[53] G. Bonnoli, F. Tavecchio, G. Ghisellini and T. Sbarrato, *An emerging population of BL Lacs with extreme properties: towards a class of EBL and cosmic magnetic field probes?*, MNRAS **451** (2015) 611 [`1501.01974`].

[54] L. Costamante, G. Bonnoli, F. Tavecchio, G. Ghisellini, G. Tagliaferri and D. Khangulyan, *The NuSTAR view on hard-TeV BL Lacs*, MNRAS **477** (2018) 4257 [`1711.06282`].

[55] A. Domínguez, J. R. Primack, D. J. Rosario, F. Prada, R. C. Gilmore, S. M. Faber et al., *Extragalactic background light inferred from AEGIS galaxy-SED-type fractions*, MNRAS **410** (2011) 2556 [`1007.1459`].

[56] L. Costamante, *Gamma-Rays from Blazars and the Extragalactic Background Light*, *International Journal of Modern Physics D* **22** (2013) 1330025 [`1309.0612`].

[57] A. Franceschini and G. Rodighiero, *The extragalactic background light revisited and the cosmic photon-photon opacity*, A&A **603** (2017) A34 [`1705.10256`].

[58] L. Costamante, *TeV-peaked candidate BL Lac objects*, *arXiv e-prints* (2019) arXiv:1911.05027 [`1911.05027`].

[59] A. Franceschini, G. Rodighiero and M. Vaccari, *Extragalactic optical-infrared background radiation, its time evolution and the cosmic photon-photon opacity*, A&A **487** (2008) 837.

[60] L. Sironi, M. Petropoulou and D. Giannios, *Relativistic jets shine through shocks or magnetic reconnection?*, MNRAS **450** (2015) 183 [`1502.01021`].

[61] M. C. Begelman, A. C. Fabian and M. J. Rees, *Implications of very rapid TeV variability in blazars*, MNRAS **384** (2008) L19 [`0709.0540`].

[62] F. Aharonian, A. G. Akhperjanian, A. R. Bazer-Bachi, B. Behera, M. Beilicke, W. Benbow et al., *An Exceptional Very High Energy Gamma-Ray Flare of PKS 2155-304*, ApJ **664** (2007) L71 [`0706.0797`].

[63] D. Giannios, D. A. Uzdensky and M. C. Begelman, *Fast TeV variability in blazars: jets in a jet*, MNRAS **395** (2009) L29 [`0901.1877`].

[64] G. Ghisellini and F. Tavecchio, *Rapid variability in TeV blazars: the case of PKS2155-304*, MNRAS **386** (2008) L28 [`0801.2569`].

[65] M. V. Barkov, F. A. Aharonian, S. V. Bogovalov, S. R. Kelner and D. Khangulyan, *Rapid TeV Variability in Blazars as a Result of Jet-Star Interaction*, ApJ **749** (2012) 119 [`1012.1787`].

[66] A. Neronov and F. A. Aharonian, *Production of TeV Gamma Radiation in the Vicinity of the Supermassive Black Hole in the Giant Radio Galaxy M87*, ApJ **671** (2007) 85 [`0704.3282`].

[67] A. Levinson and F. Rieger, *Variable TeV Emission as a Manifestation of Jet Formation in M87?*, ApJ **730** (2011) 123 [`1011.5319`].

[68] F. A. Aharonian, M. V. Barkov and D. Khangulyan, *Scenarios for Ultrafast Gamma-Ray Variability in AGN*, ApJ **841** (2017) 61 [`1704.08148`].

[69] J. Albert, E. Aliu, H. Anderhub, P. Antoranz, A. Armada, C. Baixeras et al., *Variable Very High Energy γ-Ray Emission from Markarian 501*, ApJ **669** (2007) 862 [`astro-ph/0702008`].

[70] S. Saito, Ł. Stawarz, Y. T. Tanaka, T. Takahashi, G. Madejski and F. D'Ammando, *Very Rapid High-amplitude Gamma-Ray Variability in Luminous Blazar PKS 1510-089 Studied with Fermi-LAT*, ApJ **766** (2013) L11 [`1302.0335`].

[71] J. Aleksić, L. A. Antonelli, P. Antoranz, M. Backes, J. A. Barrio, D. Bastieri et al., *MAGIC Discovery of Very High Energy Emission from the FSRQ PKS 1222+21*, ApJ **730** (2011) L8 [`1101.4645`].

[72] F. Aharonian, A. G. Akhperjanian, A. R. Bazer-Bachi, M. Beilicke, W. Benbow, D. Berge et al., *Fast Variability of Tera-Electron Volt γ Rays from the Radio Galaxy M87*, Science **314** (2006) 1424 [`astro-ph/0612016`].

[73] V. A. Acciari, E. Aliu, T. Arlen, M. Bautista, M. Beilicke, W. Benbow et al., *Radio Imaging of the Very-High-Energy γ-Ray Emission Region in the Central Engine of a Radio Galaxy*, Science **325** (2009) 444 [`0908.0511`].

[74] J. Aleksić, S. Ansoldi, L. A. Antonelli, P. Antoranz, A. Babic, P. Bangale et al., *Black hole lightning due to particle acceleration at subhorizon scales*, Science **346** (2014) 1080 [`1412.4936`].

[75] M. Kadler, D. Eisenacher, E. Ros, K. Mannheim, D. Elsässer and U. Bach, *The blazar-like radio structure of the TeV source IC 310*, A&A **538** (2012) L1 [`1201.2870`].

[76] F. A. Aharonian, M. V. Barkov and D. Khangulyan, *Scenarios for Ultrafast Gamma-Ray Variability in AGN*, ApJ **841** (2017) 61 [`1704.08148`].

[77] M. L. Lister, D. C. Homan, T. Hovatta, K. I. Kellermann, S. Kiehlmann, Y. Y. Kovalev et al., *MOJAVE. XVII. Jet Kinematics and Parent Population Properties of Relativistically Beamed Radio-loud Blazars*, ApJ **874** (2019) 43 [`1902.09591`].

[78] O. Hervet, D. A. Williams, A. D. Falcone and A. Kaur, *Probing an X-Ray Flare Pattern in Mrk 421 Induced by Multiple Stationary Shocks: A Solution to the Bulk Lorentz Factor Crisis*, ApJ **877** (2019) 26 [`1904.06802`].

[79] M. Sikora, M. C. Begelman and M. J. Rees, *Comptonization of diffuse ambient radiation by a relativistic jet: The source of gamma rays from blazars?*, ApJ **421** (1994) 153.

[80] M. C. Weisskopf, B. Ramsey, S. O'Dell, A. Tennant, R. Elsner, P. Soffitta et al., *The Imaging X-ray Polarimetry Explorer (IXPE)*, vol. 9905 of *Society of Photo-Optical Instrumentation Engineers (SPIE) Conference Series*, p. 990517. 2016. 10.1117/12.2235240.

[81] H. Zhang and M. Böttcher, *X-Ray and Gamma-Ray Polarization in Leptonic and Hadronic Jet Models of Blazars*, ApJ **774** (2013) 18 [`1307.4187`].